Transience of seawater intrusion in response to sea level rise

Ty A. Watson,[1,2] Adrian D. Werner,[1,2] and Craig T. Simmons[1,2]

Received 18 May 2010; revised 8 September 2010; accepted 6 October 2010; published 11 December 2010.

[1] Understanding seawater intrusion (SWI) induced by sea level rise (SLR) is important for the future management of many coastal aquifers. Only simplified steady state sharp interface analyses of generalized SLR-SWI exist in the literature, and the important issue of associated time scales has been neglected. We employ numerical modeling in order to explore the transience of dispersive SLR-SWI in common unconfined coastal aquifer settings. An instantaneous SLR is adopted to compare with the instantaneous sea level drop (SLD) case of a previous SLD-SWI analysis. Temporal asymmetry between the SWI responses to SLR and SLD is observed. A SLR-SWI simulation series indicates that toe "representative response times" (time to reach 95% of new steady state) range from decades to centuries for a 1 m SLR. Significant discrepancies between the representative response times of various SWI quantitative indicators (e.g., toe position, wedge center-of-mass) are observed. This demonstrates that the indication of steady state SWI conditions depends upon the monitoring approach and thus holds implications for studies reporting that SWI steady state has been attained. We adopt 100 years as a typical "planning time frame" and compare 100 year and steady state SLR-SWI. As expected, the simplified steady state sharp interface solution overpredicts the 100 year landward toe shift in most cases. However, some simulations exhibit temporary "overshoot" of the steady state interface position: this is in contradiction to the presumption that steady state SWI is the worst case. Steady state sharp interface estimates appear to be at best useful as initial approximations of SLR-SWI, given that they span 40%–250% of 100 year dispersive interface results for the cases considered.

Citation: Watson, T. A., A. D. Werner, and C. T. Simmons (2010), Transience of seawater intrusion in response to sea level rise, *Water Resour. Res.*, *46*, W12533, doi:10.1029/2010WR009564.

1. Introduction

[2] Coastal aquifers are a crucial source of freshwater for domestic, agricultural and industrial usage in many regions of the world [*Ledoux et al.*, 1990]. Changes in the coastal hydrology result in movements of the saltwater-freshwater interface [*Kim et al.*, 2009]. For example, sea level rise (SLR) driven by global climate change will induce landward migration of the saltwater-freshwater interface, i.e., seawater intrusion (SWI) [*Werner and Simmons*, 2009]. SWI threatens freshwater availability and thus a thorough understanding of SLR-induced SWI (SLR-SWI) is important for managing these resources.

[3] SWI can be analyzed using several different methods that vary in degree of complexity. The dispersive interface approach accounts for the interfacial mixing that occurs in reality, resulting in a transition zone between the freshwater and saltwater [*Bear et al.*, 1985]. This approach generally necessitates the use of variable density flow and transport numerical models. The sharp interface approximation is an alternative, more simplistic approach that assumes no mixing and thus an infinitesimally narrow boundary separating the freshwater and saltwater zones [*Bear*, 1979]. Under certain circumstances, steady state conditions are assumed to apply (e.g., where a "worst-case" condition is sought) due to advantages of parsimony and relatively small computational effort.

[4] *Werner and Simmons* [2009] adopted the most simplistic approach by employing a steady state sharp interface method to provide initial estimates of SLR-SWI. Changes in the steady state extent of SWI resulting from SLR were represented by changes in the position of the saltwater wedge "toe" (the inland extent of saline water at the aquifer basement). *Werner and Simmons* [2009] identified the hydrogeologic conditions and parameters controlling the extent of a SLR-induced landward toe shift (the difference between pre-SLR and post-SLR steady state toe positions). The main limitation of their analysis is that steady state sharp interface estimates provide a theoretical SLR-SWI extent after infinite time, i.e., time scales are neglected. It is necessary to understand the transience of SLR-SWI for the purposes of water resources planning, which typically involves finite time frames, e.g., on the order of 10 to 100 years.

[5] There are few studies that explore SWI transience in general terms. In particular, the important issue of SLR-SWI time scales remains unresolved for nonsite-specific conditions. A number of previous studies report time lags between the sea level change and the saltwater-freshwater

[1]School of the Environment, Flinders University, Adelaide, South Australia, Australia.
[2]National Centre for Groundwater Research and Training, Flinders University, Adelaide, South Australia, Australia.

0043-1397/10/2010WR009564

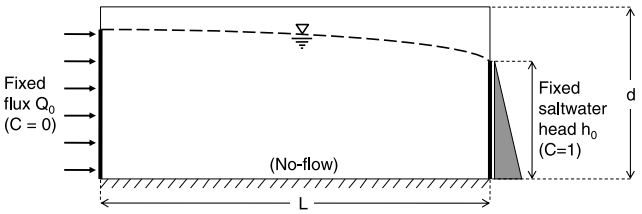

Figure 1. Schematic conceptual model of an idealized coastal aquifer system. The concentration of inflows (Q_0) through the inland boundary is $C = 0$, while ocean boundary inflows occur at seawater concentration ($C = 1$).

interface response on the order of tens of thousands and up to millions of years [e.g., *Meisler et al.*, 1984; *Essaid*, 1990; *Harrar et al.*, 2001]. These studies deal with confined aquifers and account for various site-specific complexities. *Bratton* [2007] suggests that shallow confining units found in many coastal groundwater systems may inhibit SWI. Furthermore, these previous studies all include relatively large sea level changes on geologic time scales. *Feseker* [2007] conducted a case study of a semiconfined coastal aquifer in northwestern Germany, examining the transient response to various boundary condition changes. The impact of predicted 21st century climate change-induced SLR was tested, although the single scenario examined does not allow general conclusions to be drawn. Moreover, the absolute time lag of the SWI relative to the SLR signal was not considered. Nevertheless, the single simulation by *Feseker* [2007] indicates that significant SLR-SWI is possible on much shorter time scales than reported in the aforementioned studies, with the predicted salt concentration of a 1.23 km^2 domain (subject to a SLR of 0.5 m per century) increasing by more than 11% over 250 years.

[6] A systematic study of SLR-SWI in unconfined coastal aquifers is presented in this paper. Unconfined conditions are considered because these types of aquifers are most commonly utilized for water supply purposes. Additionally, the issue of SLR-SWI is anticipated to be more urgent for unconfined coastal aquifers than for confined aquifers, as seawater encroachment in the latter is hindered by relatively slow discharge rates through the overlying low-permeability layers that are commonly associated with these systems [*Harrar et al.*, 2001].

[7] The impact of predicted 21st century global SLR is considered in this study. The simplified steady state analysis of *Werner and Simmons* [2009] is extended by considering SLR-SWI time scales and taking into account dispersive transport through transient variable density numerical simulations. The transience of SLR-SWI is assessed using a suite of quantitative indicators. Steady state-to-steady state response time scales are investigated, and the applicability of steady state sharp interface estimates of SLR-SWI to situations involving finite time frames (i.e., a water resources planning time frame of 100 years is adopted) is examined. Two key questions are posed: (1) What are the time scales associated with SLR-SWI in typical unconfined coastal aquifers, for a 1 m SLR? (2) What is the applicability of steady state sharp interface estimates of SLR-SWI for the purposes of water resources planning when compared to dispersive SWI occurring within a 100 year planning time frame?

[8] *Kiro et al.* [2008] investigated the transient response of the saltwater-freshwater transition zone to an instantaneous sea level drop (SLD) using SUTRA [*Voss*, 1984]. They developed an empirical relationship between the response time of the transition zone and various hydrogeologic parameters. Their empirical SLD-SWI relationship would theoretically be applicable also to SLR-SWI if temporal symmetry was proven to exist between the transient saltwater-freshwater interface responses to SLD and SLR. This would allow the results presented by *Kiro et al.* [2008] to be used as a proxy for SLR-SWI transience and thus be used as the basis for the present investigation. The symmetry of the transient interface responses to SLR and SLD was tested as a preliminary component of the present study. To this end, the base case results of the *Kiro et al.* [2008] SLD study were initially reproduced and subsequently compared with an equivalent SLR case.

2. Methodology

2.1. Conceptual Model

[9] The conceptual model employed for this study follows *Kiro et al.* [2008]. An idealized coastal aquifer subjected to an instantaneous SLR was considered, allowing for a comparison with the instantaneous SLD case of *Kiro et al.* [2008]. In adopting an instantaneous SLR, the SWI obtained from numerical modeling is expected to be more rapid than would occur due to gradual SLR; however this simplification provides first-order guidance on SLR-SWI transience. Infiltration recharge was neglected, as were the effects of tides and groundwater extraction.

[10] The Intergovernmental Panel on Climate Change (IPCC) predicts a 21st century SLR of 0.18–0.59 m [*Bates et al.*, 2008]. However, there exists significant disagreement among published SLR predictions, and values up to and greater than 1 m during the 21st century have been suggested [e.g., *Hansen*, 2007; *Rahmstorf*, 2007]. Due to the variability of SLR predictions, a SLR of 1 m was used throughout the SLR-SWI simulation series of the current study as an approximate representation of the order of magnitude of SLR predicted for the 21st century.

[11] The near-coastal fringe of the unconfined aquifer was represented by a rectangular, two-dimensional vertical slice perpendicular to the coast (Figure 1). The coastal boundary was approximated as a vertical face, ignoring potential landward movement of the coastline due to SLR. The ocean boundary head is $h(z) = h_0 + \alpha z$, where h_0 is the fixed ocean water level (above aquifer basement), z is the depth below h_0, and α is $(\rho_s - \rho_f)/\rho_f$, where ρ_s and ρ_f are the seawater and freshwater densities, respectively.

[12] The simplified conceptual model selected for this study allows the effects of various geometrical and hydrogeological parameters on SLR-SWI to be analyzed. The conceptual model employed also facilitates comparisons with *Kiro et al.* [2008] and *Werner and Simmons* [2009] (in particular, the analysis of the degree of temporal symmetry between SLR-SWI and SLD-SWI), allowing the current work to extend these recent contributions to the literature.

2.2. Numerical Modeling

[13] The transience of SLR-SWI was investigated via steady state-to-steady state simulations using FEFLOW

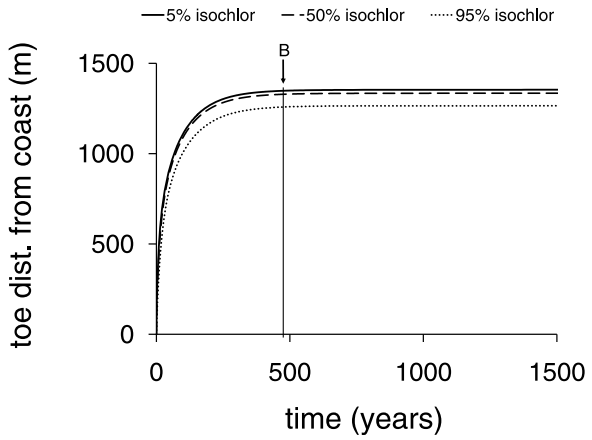

Figure 2. Example of time-marching a dispersive interface simulation to steady state conditions (parameter set 1). The transient movements of the 5%, 50%, and 95% seawater isochlors along the aquifer base are displayed. *B* is the time at which the toe rate of change falls below 0.1% of its rate of change during the first year.

[*Diersch*, 2005] and a variably saturated, density-dependent transient flow and mass transport regime. The reader is referred to *Diersch* [2005] for comprehensive documentation of the theoretical basis and development of the FEFLOW code.

[14] A constraint was imposed on the Dirichlet-type mass boundary such that seawater concentration occurred only at coastal inflow sections. This allowed freshwater and saltwater resulting from interfacial mixing to exit the domain with the ambient concentration. For computational simplicity, the development of a temporary seepage face following an instantaneous SLD was neglected in simulating the *Kiro et al.* [2008] base case. The FEFLOW simulation results are in good agreement with the results of *Kiro et al.* [2008] (results not shown for brevity), who include seepage face effects, and therefore the influence of seepage face development was considered negligible for this case.

[15] The *van Genuchten* [1980] model was adopted as the unsaturated flow parametric relationship. The initial thickness of the unsaturated zone at the coastal boundary was the same (10 m) in all simulations in order to minimize discrepancies between simulations caused by varying unsaturated zone depth.

[16] A quadrilateral mesh was employed that included a strip of vertically refined node spacings along the base of the domain to increase toe resolution and minimize the development of numerical anomalies that were observed during preliminary simulations involving a regular mesh. The transience of SLD-SWI and SLR-SWI was compared using equivalent domain dimensions to the *Kiro et al.* [2008] base case (2000 m long by 130 m deep). The number of nodes used in these simulations was selected following a grid convergence study that compared an array of quantitative indicators (5%, 50% and 95% seawater isochlors, total salt mass and wedge center-of-mass (COM)) for grids comprising 5494, 10,854, 26,934, 53,734, 134,134 and 268,134 nodes. The results obtained from grids comprising 53,734 nodes or more displayed insignificant discrepancies. The mesh of 134,134 nodes was therefore presumed to provide grid-independent solutions across the various parameter combinations, and was adopted as the preferred level of discretization. This involved node spacings of Δx = 2 m, Δz = 1 m and Δz_{base} = 0.125 m, where Δx and Δz are the horizontal and vertical element dimensions, respectively. Δz_{base} refers to the vertical dimension of the base layer of elements. The thicknesses of layers above the base layer increase by twofold in the lower 1 m. The domain size was reduced for the SLR-SWI simulation series in order to allow for a finer mesh resolution of Δx = 1 m, Δz = 0.25 m and Δz_{base} = 0.0625 m, while maintaining reasonable run times. An automatic time step control scheme was employed for all simulations, with a maximum time step size of 10 days.

2.3. Quantitative Indicators and Representative Response Times

[17] The initial conditions for SLR (or SLD) simulations were taken as the steady state conditions attained through long-term transient simulations. Steady state was deemed to have been reached when the annual rate of change of each quantitative indicator had decreased to at least 0.1% of its rate of change during the first year of simulation (e.g., see Figure 2) (in four simulations, the wedge horizontal COM exhibited minimal change during the first year, therefore the initial rate of change was taken from 1 to 2 years). In almost all cases, simulations were run for considerably longer to ensure steady state conditions were attained.

[18] The quantification of SWI transience in response to simulated SLR was based on various indicators. The 5%, 50% and 95% seawater isochlors were tracked along the aquifer base as an approximation of toe position, in a similar fashion to *Ward et al.* [2007]. The net fluid flux across the coastal boundary was adopted as a water table response indicator, following *Kiro et al.* [2008]. The net fluid flux across the coastal boundary ultimately approaches its initial value as the water table recovers to its initial hydraulic gradient after the SLR perturbation. The salt plume COM and total solute present in the domain were monitored as per the analyses of *Prasad and Simmons* [2003] and *Feseker* [2007]. Additionally, the net salt mass flux across the coastal boundary was tracked. Collectively, this suite of quantitative indicators allowed for a rigorous evaluation of SLR-SWI transience. Simulations were continued until a new steady state was attained (i.e., 1500 years in the case of Figure 2).

[19] In this study, the "representative response time" (RRT) of each quantitative indicator was defined as the time required for the quantitative indicator to reach 95% of the new steady state condition (i.e., post SLR). This was considered to be a reasonable compromise between the capture of a large portion of the steady state-to-steady state process and the magnification of potential time errors as the trends approach new steady state asymptotically. The RRT of each quantitative indicator: toe (5% seawater isochlor), total salt mass, wedge vertical COM, wedge horizontal COM, net coastal fluid flux and net coastal salt flux are denoted by τ_{toe}, τ_{mass}, $\tau_{y\text{-}COM}$, $\tau_{x\text{-}COM}$, τ_{FF} and τ_{SF}, respectively. The mathematical definition of "95% of new steady state" varies for different quantitative indicators. For some quantitative indicators, the 95% condition is assumed to occur when the quantitative indicator is within 5% of the new steady state condition (i.e., this is used for net coastal fluid flux and net coastal salt flux because initial and final values of these

Table 1. Hydrogeologic Parameters of Simulations

Parameter	Parameter Set 1	2	3	4	5	6	7	8	9	10	11	12	13	14	Units
Aquifer length (L)	2000	2000	1000	1000	1000	1000	1000	1000	1000	1000	1000	1000	2000	3000	m
Domain thickness (d)	130	130	40	40	40	40	40	40	40	20	30	45	40	40	m
Saturated thickness at the coast (h_0)	95	85	30	30	30	30	30	30	30	10	20	35	30	30	m
Inflow (per unit thickness) (Q_0)	8.2E-6	8.2E-6	1.16E-6	1.16E-6	1.16E-6	1.16E-6	9.26E-7	1.74E-6	2.31E-6	1.16E-6	1.16E-6	1.16E-6	1.16E-6	1.16E-6	m^2/s
Sea level change (Δh)	−10	+10	+1	+1	+1	+1	+1	+1	+1	+1	+1	+1	+1	+1	m
Saturated hydraulic conductivity (horizontal) (K_h)	9.91E-6	9.91E-6	8.25E-5	1.16E-5	3.47E-5	1.16E-4	8.25E-5	8.25E-5	8.25E-5	8.25E-5	8.25E-5	8.25E-5	8.25E-5	8.25E-5	m/s
Anisotropy ratio (K_v/K_h)	0.05	0.05	0.05	0.05	0.05	0.05	0.05	0.05	0.05	0.05	0.05	0.05	0.05	0.05	-
Density ratio (α)	0.23	0.23	0.025	0.025	0.025	0.025	0.025	0.025	0.025	0.025	0.025	0.025	0.025	0.025	-
Porosity (effective) (η)	0.2	0.2	0.2	0.2	0.2	0.2	0.2	0.2	0.2	0.2	0.2	0.2	0.2	0.2	-
Residual degree of saturation (s_r)	0.16	0.16	0.1	0.16	0.14	0.1	0.1	0.1	0.1	0.1	0.1	0.1	0.1	0.1	-
van Genuchten [1980] curve fitting parameter (A)	7.5	7.5	14.5	7.5	12.4	14.5	14.5	14.5	14.5	14.5	14.5	14.5	14.5	14.5	1/m
van Genuchten [1980] pore size distribution index (n)	1.89	1.89	2.68	1.89	2.28	2.68	2.68	2.68	2.68	2.68	2.68	2.68	2.68	2.68	-
Longitudinal dispersivity (β_L)	10	10	10	10	10	10	10	10	10	10	10	10	10	10	m
Transverse dispersivity (β_T)	0.01	0.01	0.01	0.01	0.01	0.01	0.01	0.01	0.01	0.01	0.01	0.01	0.01	0.01	m

Parameter	Parameter Set 15	16	17	18	19	20	21	22	23	24	25	26	27	28	Units
Aquifer length (L)	5000	1000	1000	1000	1000	1000	1000	1000	1000	1000	1000	1000	1000	2000	m
Domain thickness (d)	40	40	40	40	40	40	40	40	40	40	40	40	40	40	m
Saturated thickness at the coast (h_0)	30	30	30	30	30	30	30	30	30	30	30	30	30	30	m
Inflow (per unit thickness) (Q_0)	1.16E-6	1.16E-6	1.16E-6	1.16E-6	1.16E-6	1.16E-6	1.16E-6	1.16E-6	1.16E-6	1.16E-6	1.16E-6	1.16E-6	1.16E-6	-	m^2/s
Sea level change (Δh)	+1	+1	+1	+1	+1	+1	+1	+1	+1	+1	+1	+1	+1	+1	m
Saturated hydraulic conductivity (horizontal) (K_h)	8.25E-5	8.25E-5	8.25E-5	8.25E-5	8.25E-5	8.25E-5	8.25E-5	8.25E-5	8.25E-5	8.25E-5	8.25E-5	8.25E-5	8.25E-5	8.25E-5	m/s
Anisotropy ratio (K_v/K_h)	0.05	0.05	0.05	0.05	0.05	0.05	0.05	0.005	0.01	0.1	0.05	0.05	0.05	0.05	-
Density ratio (α)	0.025	0.025	0.025	0.025	0.025	0.025	0.025	0.025	0.025	0.025	0.025	0.025	0.025	0.025	-
Porosity (effective) (η)	0.2	0.2	0.2	0.2	0.2	0.2	0.2	0.2	0.2	0.2	0.1	0.3	0.4	0.2	-
Residual degree of saturation (s_r)	0.1	0.1	0.1	0.1	0.1	0.1	0.1	0.1	0.1	0.1	0.1	0.1	0.1	0.1	-
van Genuchten [1980] curve fitting parameter (A)	14.5	14.5	14.5	14.5	14.5	14.5	14.5	14.5	14.5	14.5	14.5	14.5	14.5	14.5	1/m
van Genuchten [1980] pore size distribution index (n)	2.68	2.68	2.68	2.68	2.68	2.68	2.68	2.68	2.68	2.68	2.68	2.68	2.68	2.68	-
Longitudinal dispersivity (β_L)	10	0.1	1	20	100	10	10	10	10	10	10	10	10	10	m
Transverse dispersivity (β_T)	0.01	0.01	0.01	0.01	0.01	0.1	1	0.01	0.01	0.01	0.01	0.01	0.01	0.01	m
Saturated thickness at the inland boundary (h_i)	-	-	-	-	-	-	-	-	-	-	-	-	-	32	m

quantitative indicators are the same). Equation (1) is used to obtain τ_{toe}, τ_{mass}, $\tau_{x\text{-}COM}$ and $\tau_{y\text{-}COM}$, (where the time variable t is equal to τ_{toe}, τ_{mass}, $\tau_{x\text{-}COM}$ or $\tau_{y\text{-}COM}$); equation (2) is used to obtain τ_{FF} and equation (3) is used to obtain τ_{SF}.

$$\frac{|X(t) - X(0)|}{|X(\infty) - X(0)|} = 0.95 \tag{1}$$

$$\frac{|Q(\tau_{FF}) - Q_0|}{Q_0} = 0.05 \tag{2}$$

$$\frac{|\Delta M(\tau_{SF})|}{|M_i(\infty)|} = 0.05 \tag{3}$$

where $X(t)$ is the value of quantitative indicator X (toe, mass, x-COM or y-COM) at time t, $X(0)$ and $X(\infty)$ are the initial steady state and post-SLR steady state values of quantitative indicator X, respectively. $Q(\tau_{FF})$ is the net fluid flux across the coastal boundary at τ_{FF}, Q_0 is the constant inflow at the inland boundary, $\Delta M(\tau_{SF})$ is the net salt mass flux across the coastal boundary at τ_{SF}, and $M_i(\infty)$ is the coastal salt mass influx at post-SLR steady state. τ_{toe} is based on the behavior of the 5% seawater isochlor due to the importance of considering the spatial extent of low salt concentrations, because water of potable quality consists of less than 1% seawater [*Voss and Souza*, 1987].

2.4. Simulation Scenarios and Parameters

[20] A series of SLR-SWI scenarios was simulated, including ranges of hydrogeologic parameters considered typical of unconfined coastal aquifers commonly used for water supply [e.g., *Werner and Gallagher*, 2006; *Kiro et al.*, 2008; *Werner and Simmons*, 2009]. Table 1 summarizes the parameters used for all numerical experiments conducted in this study. Parameter sets 1 and 2 apply to the comparison of SLD and SLR, and parameter sets 3 to 28 constitute the SLR-SWI simulation series. The base case parameters presented by *Kiro et al.* [2008] were employed in parameter sets 1 and 2. *Kiro et al.* [2008] do not state the unsaturated parameters used for their modeling, thus the mean values as reported by *Carsel and Parrish* [1988] for maximum degree of saturation s_s, residual degree of saturation s_r, *van Genuchten* [1980] curve fitting parameter A and *van Genuchten* [1980] pore size distribution n corresponding to the saturated horizontal hydraulic conductivity K_h used in the model, were adopted. *van Genuchten* [1980] unsaturated parameters were selected in this manner for both the SLD-SWI and SLR-SWI aspects of this study. Some parameters were constant across all simulations, including a storage compressibility of 2×10^{-6} m^{-1}, a maximum degree of saturation of 1 [-] and a coefficient of molecular diffusion of 10^{-9} m^2/s. A density ratio α of 0.025, which is a common representative value for the seawater-freshwater density relationship, was used throughout the SLR-SWI simulation series.

[21] *Werner and Simmons* [2009] compared flux-controlled and head-controlled systems. Their results indicate that there is potential for far more extensive SLR-SWI to occur in head-controlled systems due to the reduction in discharge to the sea caused by SLR in these cases. While we focus on the case of a constant inland flux (refer to Figure 1), one scenario involving a fixed head at the inland boundary was investigated to gain some preliminary insight into potential time scale differences for the two boundary cases (i.e., to test whether larger time scales are associated with the more extensive toe shifts of fixed head scenarios). The conceptual model (Figure 1) was modified such that Q_0 is replaced by a fixed head h_i [L] at the inland boundary (for parameter set 28). Furthermore, it was necessary to calculate τ_{FF} using equation (1) instead of equation (2) for this case, as the water table attains a new gradient at post-SLR steady state; it does not return to its initial hydraulic gradient as it does in the simulations involving a fixed flux at the inland boundary.

2.5. Steady State Sharp Interface Analysis

[22] The steady state sharp interface approximation of SWI as applied by *Werner and Simmons* [2009] was adopted for comparison with dispersive interface simulation results. *Custodio* [1987] presented the equations associated with the steady state sharp interface approximation, which are based on the Ghyben-Herzberg principle [*Baydon-Ghyben*, 1888; *Herzberg*, 1901], the Dupuit-Forchheimer approximation of horizontal flow, Darcy's Law and conservation of mass [*Werner and Simmons*, 2009]. The resulting equation for the theoretical steady state distance x_T of the toe from the coast (in the absence of recharge) is [*Custodio*, 1987]:

$$x_T = \frac{K_h \alpha (1 + \alpha) h_0^2}{2 Q_0} \tag{4}$$

Equation (4) was used to obtain sharp interface estimates of the shift in steady state toe position between pre- and post-SLR conditions.

3. Results and Discussion

3.1. Analysis of SLR Versus SLD

[23] The transient behavior of each quantitative indicator was examined for the replicated SLD base case from *Kiro et al.* [2008] (parameter set 1) and the equivalent SLR case (parameter set 2). The RRTs of all quantitative indicators are greater for the SLR case. Therefore, there exists temporal asymmetry between SLD-SWI and SLR-SWI, at least for the *Kiro et al.* [2008] conditions. We speculate that this asymmetry may be attributable to the difference in the saturated aquifer thicknesses (and therefore transmissivities) at the coastal boundary between the two cases (SLD and SLR).

[24] It appears that the results presented by *Kiro et al.* [2008] for SLD-SWI are not transferrable to SLR-SWI, at least from the single pair of SLR and SLD simulations that was considered. An assessment of the degree of temporal symmetry between SLR and SLD was not a primary objective of this study and we are careful not to suggest generality from this single result. However, this single observation of asymmetry between SLD-SWI and SLR-SWI has important ramifications, e.g., the timing of SWI and its remediation may be significantly different. In a study of a coastal aquifer in northwestern Germany, *Feseker* [2007] reports on sluggish adjustment of a simulated coastal groundwater system in response to boundary condition changes, and states that the same time scale would be

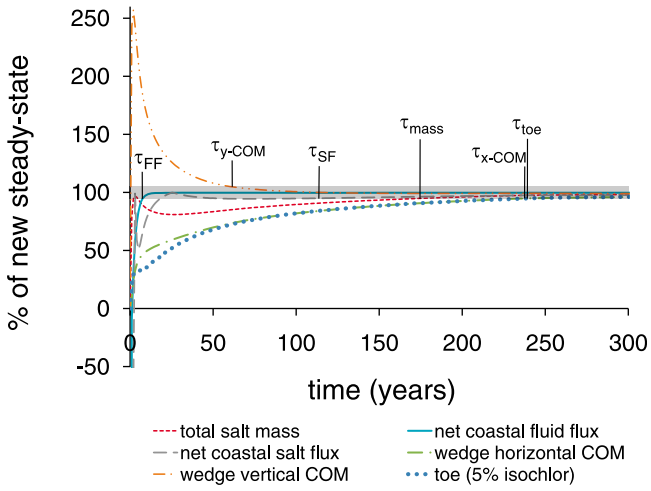

Figure 3. Temporal trends of quantitative indicators for SLR-SWI base case (parameter set 3).

expected for countermeasures to take effect. The results of the current study indicate that further analysis of the *Feseker* [2007] situation is required before symmetry/asymmetry can be presumed in that case. A more systematic investigation beyond the single situation assessed here is required before more general conclusions regarding SWI asymmetry can be drawn.

3.2. Analysis of SLR-SWI

[25] A series of hypothetical SLR-SWI situations that are simple deviations from a base case (parameter set 3) were simulated to evaluate SLR-SWI for different hydrogeological conditions. Model run times were large (typically 100 h per simulation), which constrained the number of cases that were tested and precluded a rigorous sensitivity analysis. Figure 3 displays the transient behavior of each quantitative indicator for the base case. All trends are represented as a percentage of new steady state relative to the pre-SLR steady state. The shaded region represents conditions that are within 5% of post-SLR steady state.

[26] In Figure 3, there is a notable sequencing of the various quantitative indicators. Furthermore, some quantitative indicators follow a simple asymptotic trend, while others exhibit wave-like fluctuations. For example, the wedge vertical COM exceeds its new steady state value and subsequently approaches steady state from values greater than 100% of the steady state-to-steady state change. For such cases throughout the present study, 105% (as a surrogate for 95%) of post-SLR steady state was used to obtain the RRT.

3.2.1. SLR-SWI Time Scales

[27] Figure 4 displays the RRTs of the six quantitative indicators for 26 different parameter combinations. For clarity, the results are ordered according to the τ_{toe} values – from most rapid to slowest.

[28] There is a somewhat consistent sequence in the RRTs of various quantitative indicators. For example, τ_{toe} is greater than $\tau_{y\text{-}COM}$ in all but one simulation, which indicates that the depth to the saltwater wedge consistently responds more rapidly than the toe. The RRT sequence is exemplified by the averages across the 26 simulations, which for τ_{FF}, $\tau_{y\text{-}COM}$, τ_{SF}, τ_{mass}, $\tau_{x\text{-}COM}$ and τ_{toe} are 10 years, 70 years, 100 years, 150 years, 190 years and 190 years, respectively.

[29] There are some deviations from the general sequence of RRTs in Figure 4. For example, a relatively large τ_{SF} occurs for the single simulation that involves a fixed head at the inland boundary (parameter set 28). More simulations with this boundary condition are required to establish whether τ_{SF} values are consistently larger in head-controlled settings. The simulation with the lowest K (parameter set 4) produced an anomalously high $\tau_{y\text{-}COM}$. This case involves

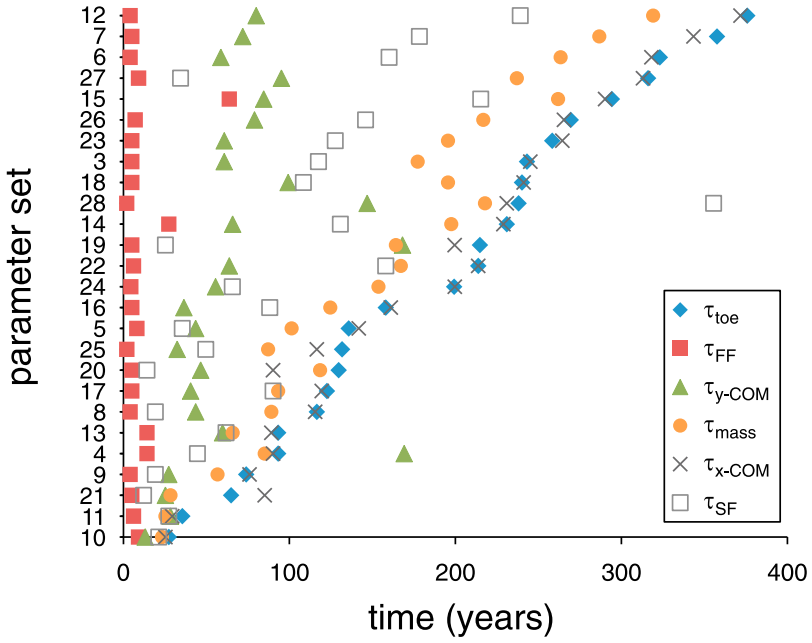

Figure 4. RRTs of quantitative indicators for the SLR-SWI simulation series.

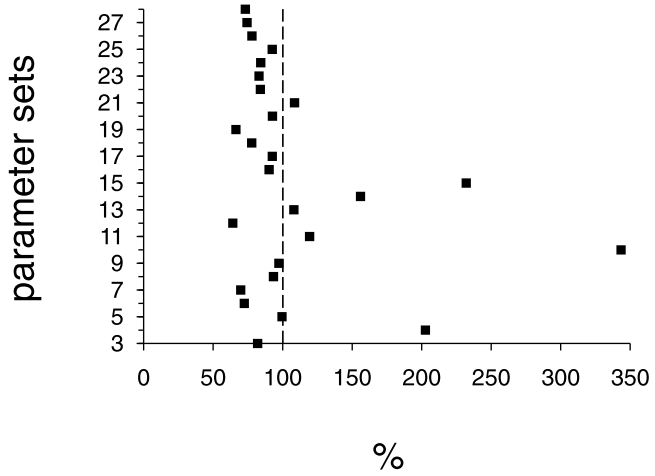

Figure 5. Comparison of simulated 100 year maximum toe shift and simulated steady state-to-steady state toe shift. One hundred year maxima are represented as a percentage of steady state-to-steady state values.

the smallest landward toe shift of just 7 m, and it is also the only case in which the vertical COM is lower in post-SLR conditions than in pre-SLR conditions. Individual indicator trends are difficult to interpret without extensive characterization of each SLR-SWI case, and variability between cases is indicative of the complex relationships that exist between parameters and the SWI response to SLR. Nonetheless, we contend that there is sufficient consistency in the results to provide general insight into SLR-SWI transience.

[30] The τ_{toe} range in Figure 4 indicates that typical time scales for SWI induced by anticipated 21st century SLR are on the order of decades and centuries, for the tested cases. This result is compatible with the single simulation of SLR-SWI in a semiconfined coastal aquifer by *Feseker* [2007]. *Rozell and Wong* [2010] investigated the effects of future climate change scenarios on the saltwater-freshwater interface beneath Shelter Island. The hydrogeologic parameters considered in the present study are somewhat comparable with those of the Shelter Island system. Direct comparisons are difficult due to consideration of the joint effects of sea level rise and recharge change by *Rozell and Wong* [2010]. Nonetheless, the 0.61 m sea level rise scenario investigated by these authors (which also involved a 2% recharge reduction) resulted in landward shifts in the potable water interface (approximately the 1% seawater isochlor) of comparable magnitudes to the range of toe shifts observed for the fixed flux simulations in the present study (on the order of tens of meters). *Rozell and Wong* [2010] did not report on the time scales associated with the saltwater-freshwater interface movement beneath Shelter Island in response to the simulated climate change perturbations. It would be reasonable to expect similar time scales to those observed in the present study.

[31] In most cases, the toe takes longer than 100 years to respond to the instantaneous SLR. This indicates that landward migration of the toe due to a 1 m SLR occurring in 100 years is unlikely to maintain a quasi steady state condition due to the SWI time lag. While SWI is often quantified by movements of the saltwater wedge toe [e.g., *Werner and Simmons*, 2009], relevant time scales for SWI may be better represented by other quantitative indicators, depending on the situation. The connotations associated with the sequencing of the RRTs of the various SWI quantitative indicators are discussed further in section 3.2.2.

[32] A constant inland head scenario was undertaken to briefly examine SLR-SWI time scales subject to an alternative inland boundary condition. The simulated steady state-to-steady state toe shift for this case (parameter set 28) was 560 m, which exceeds the maximum toe shift observed in the 25 constant inland flux simulations by tenfold. This result is in agreement with *Werner and Simmons* [2009], who suggest that the case of a fixed head at the inland boundary produces far greater landward toe shifts when compared to a corresponding constant inland flux case. Despite the more extensive toe shift of the fixed inland head scenario, the associated τ_{toe} of 240 years is well within the spread of τ_{toe} values for the constant inland flux simulations (parameter sets 3 to 27). The τ_{toe} value for parameter set 2 (10 m SLR simulation) of 220 years is also well within the range of values obtained from the 1 m SLR-SWI simulations (parameter sets 3 to 28). From these results, it would appear that the relationships between SLR-SWI time scales and such factors as the magnitude of SLR and the total landward shift of the toe are not linear.

3.2.2. Sequencing of SWI Quantitative Indicator RRTs

[33] The assessment of time scales indicates that the time for attainment of steady state conditions (i.e., as inferred from RRTs; Figure 4) varies markedly between quantitative indicators. This highlights the need for careful selection of a quantitative indicator pertaining to the issue of interest. The steady state indicators of total salt mass and transition zone characteristic time used by *Feseker* [2007] and *Kiro et al.* [2008], respectively, are expected to underestimate the time required for the toe to reach steady state conditions.

[34] There are potential practical implications of the differences between $\tau_{y\text{-}COM}$ and τ_{toe}. As $\tau_{y\text{-}COM}$ values are typically significantly smaller than τ_{toe} values, well salinization from SLR-SWI caused by a vertical rise in the saltwater-freshwater interface (e.g., impacting on shallow skimming wells) may occur sooner than the salinization of wells inland of the toe. Also, the location of the toe is often inferred by a limited number of saltwater-freshwater interface depth measurements [*Melloul and Zeitoun*, 1999], which may be rather poor indicators of the steady state toe location under transient conditions.

3.3. Steady State Versus 100 Year SLR-SWI

3.3.1. Transient Overshoot of Steady State SWI

[35] Figure 5 displays a comparison of 100 year maximum toe shifts and steady state toe shifts for the SLR-SWI simulation series. The maximum toe shift occurring within the first 100 years is presented as a percentage of the steady state-to-steady state toe shift.

[36] Most data points in Figure 5 lie between 65% and 100%, indicating cases where the toe remains seaward of the new steady state location after 100 years of simulation. Surprisingly, values greater than 100% are also observed. These points indicate cases in which a temporary landward "overshoot" of the new steady state toe location occurs. The overshoot of the toe is significant in some cases, with the new steady state location being exceeded by up to approximately 250%. Previous studies of SLR-SWI consider the post-SLR steady state saltwater-freshwater interface position

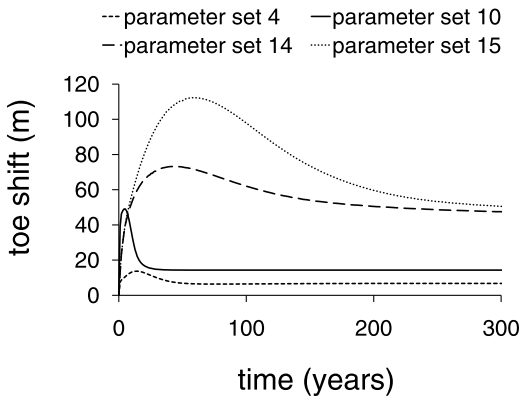

Figure 6. Toe shift trends showing the overshoot phenomenon.

and adopt this as the worst case of inland extent of saltwater contamination due to SLR [e.g., *Sherif and Singh*, 1999; *Werner and Simmons*, 2009]. From the perspective of water resources planning, the potential of SWI extending beyond the steady state position is an important consideration. Figure 6 displays four transient toe shift trends that exemplify the overshoot phenomenon.

[37] *Kiro et al.* [2008] observed some instances of "back and forth movement" of the transition zone in response to an instantaneous SLD, although the scale of this effect was not defined. This is reported to have occurred for cases involving a large water table response time relative to the transition zone response time. *Kiro et al.* [2008] quantified water table response time via the "groundwater characteristic time," which is based on the time constant for a groundwater system as defined by *Domenico and Schwartz* [1998], given by

$$T_c = \frac{S_y L^2}{bK} \tag{5}$$

where T_c is the time constant [T], S_y is specific yield [-], and b is the thickness of the system [L]. We examined the relationship between T_c and SWI overshoot using time-integrated overshoot I_o (m · years) as a measure of overshoot magnitude, defined as

$$I_o = \int_{t_1}^{\tau_{toe}} (x_T(t) - x_{Tss})\, dt \tag{6}$$

where t_1 is the time at which the toe initially overshoots the steady state position [T], $x_T(t)$ is the transient position [L] of the toe at time t obtained through FEFLOW modeling, and x_{Tss} is the post-SLR steady state toe position [L] obtained through FEFLOW modeling. Figure 7 displays the relationship between T_c (with h_0 used as a proxy for b) and I_o, for the simulations in which overshoot occurred. Values of T_c for which no overshoot occurred (which cannot be displayed on the logarithmic scale, as $I_o = 0$) were relatively low (≤3.8 years).

[38] The T_c-I_o relationship shown in Figure 7 indicates a greater potential for overshoot for higher values of T_c. In the simulations conducted for this study, the SLR generates a water table wave that propagates at a rate determined by T_c and, in cases involving a fixed flux at the inland boundary, controls the time required for the water table to return to its original hydraulic gradient. The SLR-induced water table wave eventually causes the head at the inland boundary to rise in fixed flux cases, reflecting the constant hydraulic gradient imposed at the inland boundary. Larger values of T_c are therefore associated with simulations in which the SLR-induced water table wave imposes hydraulic controls on the system for longer durations; i.e., prior to the reinstatement of steady state flow conditions. The sustained periods of flow field perturbation in high T_c simulations are those in which overshoot is most likely to occur. T_c is obtained from the diffusion equation for fluid flow and is therefore associated with only the advective aspects of the system [*Domenico and Schwartz*, 1998]; i.e., T_c does not account for variable density flow. A correlation between T_c and saltwater dynamics is observed in this study because the horizontal migration of the saltwater wedge is influenced by the water table wave generated by the instantaneous SLR.

[39] The generation of the water table wave is enhanced by the instantaneous nature of the SLR, thus the question of whether it is plausible for overshoot to occur in response to gradual SLR remains a topic of future inquiry. Regardless of whether overshoot is plausible under gradual SLR conditions, it is expected that the scenarios for which overshoot occurs would at least correspond to relatively rapid toe responses in the gradual SLR case. Therefore, more generally, the increase in T_c with I_o indicates that the toe is likely to respond more rapidly to SLR for greater values of T_c.

[40] Other factors were assessed to test for correlations with I_o, including hydraulic gradient (defined as $Q_0/K_h h_0$) and dispersion effects, quantified as changes in transition zone width. There was no clear relationship between hydraulic gradient and overshoot. Transition zone widening (defined as the increase in distance between the 5% and 95% seawater isochlors at the aquifer basement) was less than overshoot distance for five of the seven occurrences of SWI overshoot, and therefore the overshoot phenomenon appears to be driven by both advective and dispersive processes.

[41] Further work is recommended to investigate the plausibility of overshoot occurring in real world settings. *Goswami and Clement* [2007] conducted experiments in a laboratory-scale porous media tank in order to study seawater intrusion transience. A similar experimental setup, with a fixed flux inland boundary and a large tank

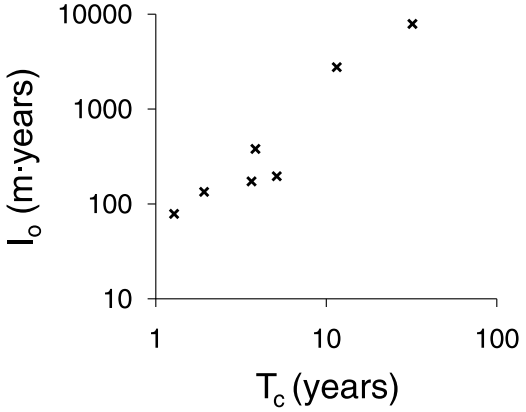

Figure 7. Log plot of the relationship between the groundwater system time constant T_c and integrated overshoot I_o.

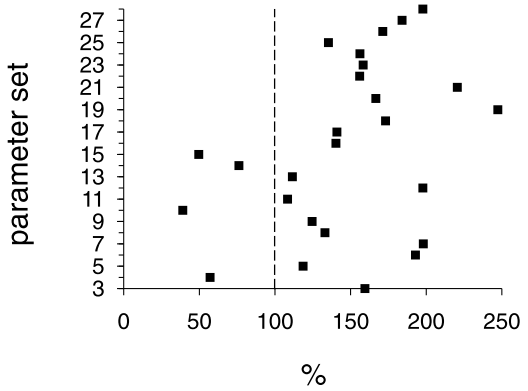

Figure 8. Steady state sharp interface toe shift estimates as a percentage of simulated 100 year maximum dispersive interface toe shifts.

length-to-depth ratio in order to achieve a large T_c value, could be used to attempt to demonstrate SLR-SWI overshoot in a physical experiment.

3.3.2. Applicability of Steady State Sharp Interface Estimates to Planning Time Frames

[42] The steady state-to-steady state toe shifts yielded from the dispersive interface simulations were compared with the steady state sharp interface estimates of toe shift. It has been established in the literature that the sharp interface method tends to overestimate dispersive interface SWI extent [*Volker and Rushton*, 1982]. However, to the authors' knowledge, pre- to post-SLR toe shifts from the two methods have not been compared. It is observed that the sharp interface method overestimates the simulated steady state-to-steady state toe shifts by between 15% and 139%, with an average of 35%, for the cases considered.

[43] The applicability of steady state sharp interface estimates of SLR-SWI for approximating dispersive SLR-SWI occurring within a 100 year planning time frame was also assessed. Figure 8 presents each steady state sharp interface estimate as a percentage of the simulated dispersive interface 100 year maximum toe shift.

[44] Figure 8 shows that steady state sharp interface toe shift estimates vary from approximately 40% to approximately 250% of the simulated dispersive interface 100 year maximum toe shifts for the considered SLR-SWI scenarios. This range alone is sufficient to demonstrate the potential inaccuracy of 100 year SLR-SWI predictions from application of the steady state sharp interface method. Furthermore, it indicates that the steady state sharp interface method may in fact underestimate dispersive interface toe shift in certain situations – a result of the overshoot phenomenon discussed in section 3.3.1. This contradicts the common assumption that the sharp interface method always overestimates true toe penetration and thus can be generally relied upon to provide SWI estimates that are on the safe side for water resources planning [e.g., *Custodio*, 1987].

4. Conclusions

[45] The transience of SLR-SWI in typical unconfined coastal aquifer settings was explored using variable density numerical modeling. SLR-SWI transience was quantified by monitoring the temporal behavior of six different SWI quantitative indicators from the simulations. A simplified conceptual framework comprising homogeneous aquifer conditions and constant aquifer stresses was considered in order to extend the findings of recent studies concerning the SWI response to sea level changes. The simplified nature of the analysis precludes various complicating factors that are common in coastal aquifer settings, such as short-duration fluctuations in the saltwater-freshwater interface position due to tidal forcing and seasonal recharge variability [e.g., *Michael et al.*, 2005], among other hydrogeological complexities. It is recommended that future investigation be undertaken that considers the influences of spatial variability in aquifer properties (including confining layers), seawater inundation of the land surface due to SLR and the resultant potential for convective fingering (e.g., as investigated by *Kooi et al.* [2000] in the context of geologic time scales), and the effects of groundwater extraction and three dimensionality.

[46] Transient asymmetry between SLD-SWI and SLR-SWI was observed in modeling results, and therefore the SLD-SWI relationships obtained from the previous study by *Kiro et al.* [2008] are not transferrable to the SLR case. While only a single case was tested, this conveys the need to treat SLD and SLR individually and demonstrates that temporal symmetry cannot be presumed between the advance and retreat of the saltwater-freshwater interface in response to sea level changes.

[47] The results of 26 SLR simulations indicate that typical time scales for toe migration in response to a 1 m SLR range from decades to centuries for typical unconfined coastal aquifer settings. However, the time scales vary significantly depending upon which quantitative indicator is considered. For example, $\tau_{y\text{-}COM}$ is significantly smaller than τ_{toe} in most simulations, τ_{mass} and τ_{SF} are generally smaller than τ_{toe}, and τ_{FF} always precedes the response times of all other analyzed quantitative indicators. The contrast in time scales highlights the need for careful selection of the quantitative indicator for assessing SWI transience; consideration should be given to the SWI processes that are of greatest importance.

[48] There is some evidence that SLR-SWI time scales are not linearly related to the SLR or toe shift magnitudes. Despite significantly larger toe shifts, the τ_{toe} values for both the single fixed inland head scenario and the *Kiro et al.* [2008] base case involving a 10 m SLR lie well within the range of τ_{toe} values obtained from the SLR-SWI simulation set involving a fixed inland flux and a 1 m SLR.

[49] Temporary overshoot of the post-SLR steady state toe position (obtained from dispersive SWI simulation) by up to 250% is observed in several of the simulated scenarios. Results indicate greater potential for more rapid toe response, possibly leading to overshoot, for higher values of the groundwater system time constant T_c. The overshoot phenomenon contradicts the common assumption that steady state is the worst case for inland SWI extent arising through SLR. The occurrence of overshoot causes sharp interface steady state estimates of SWI to underpredict the simulated 100 year SWI extent in some cases. Therefore, the steady state sharp interface method may not always provide SWI estimates that are conservative for water resources planning. The steady state sharp interface estimates of toe shift span 40–250% of the toe shifts obtained from the 100 year dispersive interface simulations. This large range

indicates that steady state sharp interface estimates are at best only crude initial estimates of 100 year SLR-SWI.

[50] **Acknowledgments.** The authors wish to thank Yael Kiro (Hebrew University of Jerusalem) for provision of SUTRA modeling files. We gratefully acknowledge James Ward (University of South Australia) and Yueqing Xie (Flinders University) for their FEFLOW modeling/programming assistance. We thank the reviewers for their constructive comments that helped improve the paper. Author Ty Watson was supported by an SA Water Honors scholarship and the work was funded by the National Centre for Groundwater Research and Training, a collaborative initiative of the Australian Research Council and the National Water Commission.

References

Bates, B. C., Z. W. Kundzewicz, S. Wu, and J. P. Palutikof (2008), Climate change and water, *Tech. Pap. VI*, 210 pp., IPCC Secr., Geneva, Switz.

Baydon-Ghyben, W. B. (1888), *Nota in Verband Met de Voorgenomen Putboring Nabij Amsterdam*, pp. 8–22, K. Inst. Ing. Tijdschrift, The Hague, Neth.

Bear, J. (1979), *Hydraulics of Groundwater*, 569 pp., McGraw-Hill, New York.

Bear, J., U. Shamir, A. Gamliel, and A. M. Shapiro (1985), Motion of the seawater interface in a coastal aquifer by the method of successive steady states, *J. Hydrol.*, *76*, 119–132, doi:10.1016/0022-1694(85)90093-9.

Bratton, J. F. (2007), The importance of shallow confining units to submarine groundwater flow, in *A New Focus on Groundwater-Seawater Interactions*, *IAHS Proceedings and Reports*, vol. 312, edited by W. Sanford et al., pp. 28–36, IAHS Press, Wallingford, U. K.

Carsel, R. F., and R. S. Parrish (1988), Developing joint probability distributions of soil water retention characteristics, *Water Resour. Res.*, *24*, 755–769, doi:10.1029/WR024i005p00755.

Custodio, E. (1987), Prediction methods, in *Groundwater Problems in Coastal Areas: A Contribution to the International Hydrological Programme*, *Studies and Reports in Hydrology*, vol. 45, edited by G. A. Bruggeman and E. Custodio, chap. 8, pp. 344–345, UNESCO, Paris.

Diersch, H.-J. G. (2005), *FEFLOW Reference Manual*, 292 pp., WASY Ltd., Berlin.

Domenico, P. A., and F. W. Schwartz (1998), *Physical and Chemical Hydrogeology*, 2nd ed., 506 pp., John Wiley, New York.

Essaid, H. I. (1990), A multilayered sharp interface model of coupled freshwater and saltwater flow in coastal systems: Model development and application, *Water Resour. Res.*, *26*, 1431–1454, doi:10.1029/WR026i007p01431.

Feseker, T. (2007), Numerical studies on saltwater intrusion in a coastal aquifer in northwestern Germany, *Hydrogeol. J.*, *15*, 267–279, doi:10.1007/s10040-006-0151-z.

Goswami, R. R., and T. P. Clement (2007), Laboratory-scale investigation of saltwater intrusion dynamics, *Water Resour. Res.*, *43*, W04418, doi:10.1029/2006WR005151.

Hansen, J. E. (2007), Scientific reticence and sea level rise, *Environ. Res. Lett.*, *2*, 024002, doi:10.1088/1748-9326/2/2/024002.

Harrar, W. G., A. T. Williams, J. A. Barker, and M. V. Camp (2001), Modeling scenarios for the emplacement of palaeowaters on aquifer systems, in *Palaeowaters in Coastal Europe: Evolution of Groundwater Since the Late Pleistocene*, *Spec. Publ.* vol. 189, edited by W. M. Edmunds and C. J. Milne, pp. 213–229, Geol. Soc. of London, London.

Herzberg, A. (1901), Die Wasserversorgung einiger Nordseebäder, *J. Gasbeleucht. Verw. Beleuchtungsarten Wasserversorg.*, *44*, 815–844.

Kim, K.-Y., Y.-S. Park, G.-P. Kim, and K.-H. Park (2009), Dynamic freshwater-saline water interaction in the coastal zone of Jeju Island, South Korea, *Hydrogeol. J.*, *17*, 617–629, doi:10.1007/s10040-008-0372-4.

Kiro, Y., Y. Yechieli, V. Lyakhovsky, E. Shalev, and A. Starinsky (2008), Time response of the water table and saltwater transition zone to a base level drop, *Water Resour. Res.*, *44*, W12442, doi:10.1029/2007WR006752.

Kooi, H., J. Groen, and A. Leijnse (2000), Modes of seawater intrusion during transgressions, *Water Resour. Res.*, *36*, 3581–3589, doi:10.1029/2000WR900243.

Ledoux, E., S. Sauvagnac, and A. Rivera (1990), A compatible single-phase/two-phase numerical model: 1. Modeling the transient salt-water/fresh-water interface motion, *Ground Water*, *28*, 79–87, doi:10.1111/j.1745-6584.1990.tb02231.x.

Meisler, H., P. P. Leahy, and L. L. Knobel (1984), Effect of eustatic sea-level changes on saltwater freshwater relations in the northern Atlantic coastal plain, *U.S. Geol. Surv. Water Supply Pap.*, *2255*, 28 pp.

Melloul, A. J., and D. G. Zeitoun (1999), A semi-empirical approach to intrusion monitoring in Israeli coastal aquifer, in *Seawater Intrusion in Coastal Aquifers: Concepts, Methods and Practices*, edited by J. Bear et al., pp. 543–558, Kluwer Acad., Dordrecht, Neth.

Michael, H. A., A. Mulligan, and C. F. Harvey (2005), Seasonal water exchange between aquifers and the coastal ocean, *Nature*, *436*, 1145–1148, doi:10.1038/nature03935.

Prasad, A., and C. T. Simmons (2003), Unstable density-driven flow in heterogeneous porous media: A stochastic study of the Elder [1967b] "short heater" problem, *Water Resour. Res.*, *39*(1), 1007, doi:10.1029/2002WR001290.

Rahmstorf, S. (2007), A semi-empirical approach to projecting future sea-level rise, *Science*, *315*, 368–370, doi:10.1126/science.1135456.

Rozell, D. J., and T.-f. Wong (2010), Effects of climate change on groundwater resources at Shelter Island, New York State, USA, *Hydrogeol. J.*, *18*, doi:10.1007/s10040-010-0615-z.

Sherif, M. M., and V. P. Singh (1999), Effect of climate change on sea water intrusion in coastal aquifers, *Hydrol. Processes*, *13*, 1277–1287, doi:10.1002/(SICI)1099-1085(19990615)13:8<1277::AID-HYP765>3.0.CO;2-W.

van Genuchten, M. T. (1980), A closed-form equation for predicting the hydraulic conductivity of unsaturated soils, *Soil Sci. Soc. Am. J.*, *44*, 892–898, doi:10.2136/sssaj1980.03615995004400050002x.

Volker, R. E., and K. R. Rushton (1982), An assessment of the importance of some parameters for seawater intrusion in aquifers and a comparison of dispersive and sharp interface modeling approaches, *J. Hydrol.*, *56*, 239–250, doi:10.1016/0022-1694(82)90015-4.

Voss, C. I. (1984), SUTRA: Finite-element simulation model for saturated-unsaturated, fluid-density-dependent groundwater flow with energy transport or chemically reactive single-species solute transport, *U.S. Geol. Surv. Water Resour. Invest. Rep.*, *84-4369*, 429 pp.

Voss, C. I., and W. R. Souza (1987), Variable density flow and solute transport simulation of regional aquifers containing a narrow saltwater-freshwater transition zone, *Water Resour. Res.*, *23*, 1851–1866, doi:10.1029/WR023i010p01851.

Ward, J. D., C. T. Simmons, and P. J. Dillon (2007), A theoretical analysis of mixed convection in aquifer storage and recovery: How important are density effects?, *J. Hydrol.*, *343*, 169–186, doi:10.1016/j.jhydrol.2007.06.011.

Werner, A. D., and M. R. Gallagher (2006), Characterisation of sea-water intrusion in the Pioneer Valley, Australia using hydrochemistry and three-dimensional numerical modeling, *Hydrogeol. J.*, *14*, 1452–1469, doi:10.1007/s10040-006-0059-7.

Werner, A. D., and C. T. Simmons (2009), Impact of sea-level rise on sea water intrusion in coastal aquifers, *Ground Water*, *47*, 197–204, doi:10.1111/j.1745-6584.2008.00535.x.

C. T. Simmons, T. A. Watson, and A. D. Werner, National Centre for Groundwater Research and Training, Flinders University, GPO Box 2100, Adelaide, SA 5001, Australia. (craig.simmons@flinders.edu.au; ty.watson@flinders.edu.au; adrian.werner@flinders.edu.au)